Evaluation of two-photon exchange graphs for excited states of highly charged heliumlike ions

Peter J. Mohr
National Institute of Standards and Technology, Gaithersburg, Maryland 20899

J. Sapirstein
Department of Physics, University of Notre Dame, Notre Dame, Indiana 46556

(Received 12 May 2000; revised manuscript received 22 June 2000; published 9 October 2000)

Energy shifts arising from two-photon-exchange graphs are calculated for $n=2$ triplet states of heliumlike ions and tabulated for the range of nuclear charges $Z=30-92$. The results are compared with second-order many-body perturbation theory (MBPT), and the differences are identified as QED effects associated with retardation and negative energy states not included in MBPT.

PACS number(s): 31.25.Jf, 31.30.Jv, 12.20.Ds

I. INTRODUCTION

S-matrix theory [1] provides a systematic approach to the calculation of the properties of highly charged ions in a way that includes both correlation and QED effects. The method has been applied [2,3] to the calculation of two-photon exchange diagrams for the ground state of heliumlike ions, and more recently to the calculation of vertex corrections in that state [4]. While the ground state is of experimental interest [5], much more data are available for transitions involving the $n=2$ excited states. In this paper we extend the treatment of Ref. [2] to these states. While the basic formalism is essentially the same as applied to the ground state, there are two novel features to the calculation. The first has to do with the more complicated structure of cuts associated with the photon propagators in the complex plane. This leads to the introduction of new integrals around contours not present in the ground-state calculation. The second has to do with reference-state contributions [6], which have a considerably more complicated structure than in the ground-state case, and play a more important numerical role.

The plan of the paper is the following. Section II presents the basic equations for the energy shifts arising from two-photon exchange for excited states of heliumlike ions in which one electron is in the ground state. In Sec. III, we numerically evaluate these corrections for $n=2$ states, and in the final section we compare these results with the approximate treatment provided by many-body perturbation theory (MBPT).

II. FORMALISM

In *S*-matrix theory, the fourth-order energy is

$$E^{(4)}=\lim_{\epsilon\to 0}\frac{i\epsilon}{2}\left[4\langle S_\epsilon^{(4)}\rangle_c-2\langle S_\epsilon^{(2)}\rangle_c^2\right]. \tag{1}$$

The subscript c means only connected diagrams are included, and

$$S_\epsilon=T\left(e^{-ie\int d^4x\, e^{-\epsilon|x_0|}\bar{\psi}(x)\gamma_\mu\psi(x)A^\mu(x)}\right). \tag{2}$$

In this paper we consider two-photon exchange contributions to $S_\epsilon^{(4)}$ where the photons are either uncrossed (L),

$$\begin{aligned}\langle S_\epsilon^{(4)}\rangle_{\rm L}=&\frac{8\alpha^2}{\pi^2}\int d\mathbf{x}_4\int d\mathbf{x}_3\int d\mathbf{x}_2\int d\mathbf{x}_1\int_{-\infty}^{\infty}dq_2\int_{-\infty}^{\infty}dq_1\\&\times\int_{-\infty}^{\infty}dz_2\int_{-\infty}^{\infty}dz_1\sum_{n_4n_3n_2n_1}\langle a_{n_4}^\dagger a_{n_2}^\dagger a_{n_1}a_{n_3}\rangle\\&\times\frac{\epsilon}{\epsilon^2+(E_{n_4}-z_2-q_2)^2}\,\frac{\epsilon}{\epsilon^2+(E_{n_3}-z_2+q_1)^2}\\&\times\frac{\epsilon}{\epsilon^2+(E_{n_2}-z_1+q_2)^2}\,\frac{\epsilon}{\epsilon^2+(E_{n_1}-z_1-q_1)^2}\\&\times\phi_{n_4}^\dagger(\mathbf{x}_4)\alpha_\mu G(\mathbf{x}_4,\mathbf{x}_3,uz_2)\alpha_\nu\phi_{n_3}(\mathbf{x}_3)\\&\times H(\mathbf{x}_4-\mathbf{x}_2,q_2)\phi_{n_2}^\dagger(\mathbf{x}_2)\alpha^\mu G(\mathbf{x}_2,\mathbf{x}_1,uz_1)\\&\times\alpha^\nu\phi_{n_1}(\mathbf{x}_1)H(\mathbf{x}_3-\mathbf{x}_1,q_1),\end{aligned} \tag{3}$$

or crossed (X),

$$\begin{aligned}\langle S_\epsilon^{(4)}\rangle_{\rm X}=&\frac{8\alpha^2}{\pi^2}\int d\mathbf{x}_4\int d\mathbf{x}_3\int d\mathbf{x}_2\int d\mathbf{x}_1\int_{-\infty}^{\infty}dq_2\int_{-\infty}^{\infty}dq_1\\&\times\int_{-\infty}^{\infty}dz_2\int_{-\infty}^{\infty}dz_1\sum_{n_4n_3n_2n_1}\langle a_{n_4}^\dagger a_{n_2}^\dagger a_{n_1}a_{n_3}\rangle\\&\times\frac{\epsilon}{\epsilon^2+(E_{n_4}-z_2-q_2)^2}\,\frac{\epsilon}{\epsilon^2+(E_{n_3}-z_2+q_1)^2}\\&\times\frac{\epsilon}{\epsilon^2+(E_{n_2}-z_1+q_1)^2}\,\frac{\epsilon}{\epsilon^2+(E_{n_1}-z_1-q_2)^2}\\&\times\phi_{n_4}^\dagger(\mathbf{x}_4)\alpha_\mu G(\mathbf{x}_4,\mathbf{x}_3,uz_2)\alpha_\nu\phi_{n_3}(\mathbf{x}_3)\\&\times H(\mathbf{x}_4-\mathbf{x}_1,q_2)\phi_{n_2}^\dagger(\mathbf{x}_2)\alpha^\nu G(\mathbf{x}_2,\mathbf{x}_1,uz_1)\\&\times\alpha^\mu\phi_{n_1}(\mathbf{x}_1)H(\mathbf{x}_3-\mathbf{x}_2,q_1),\end{aligned} \tag{4}$$

where $u=1+i\delta$. We will refer to these henceforth as the ladder (L) and crossed ladder (X) terms. In the above expressions, the photon Green's function is given by

$$H(\vec{r},z)=-\frac{e^{-b|\vec{r}|}}{4\pi|\vec{r}|},\tag{5}$$

where $b=-i\sqrt{z^2+i\delta}$, $\mathrm{Re}(b)>0$, and the electron Green's function has the spectral representation

$$G(\vec{x}_2,\vec{x}_1,uz)=\sum_i \frac{\phi_i(\vec{x}_2)\phi_i^\dagger(\vec{x}_1)}{E_i-uz}.\tag{6}$$

We also have

$$\begin{aligned}\langle S_\epsilon^{(2)}\rangle_{\mathrm{E}}=4i\alpha\int d\mathbf{x}_2\int d\mathbf{x}_1\int_{-\infty}^{\infty}dq \sum_{n_4n_3n_2n_1}\langle a_{n_4}^\dagger a_{n_2}^\dagger a_{n_1}a_{n_3}\rangle\\ \times\frac{\epsilon}{\epsilon^2+(E_{n_4}-E_{n_3}-q)^2}\,\frac{\epsilon}{\epsilon^2+(E_{n_2}-E_{n_1}+q)^2}\\ \times\phi_{n_4}^\dagger(\mathbf{x}_2)\alpha_\mu\phi_{n_3}(\mathbf{x}_2)\phi_{n_2}^\dagger(\mathbf{x}_1)\\ \times\alpha^\mu\phi_{n_1}(\mathbf{x}_1)H(\mathbf{x}_2-\mathbf{x}_1,q).\end{aligned}\tag{7}$$

We specialize here to the case of two-electron atoms with zero-order states of the form

$$F_{va}a_v^\dagger a_a^\dagger|0\rangle,\tag{8}$$

where a is taken to represent a $1s$ orbital with energy E_a and magnetic quantum number μ_a, and v is taken to represent an excited orbital with energy E_v and magnetic quantum number μ_v. A combination of these energies we will use frequently in this paper is

$$E_v-E_a\equiv\delta E.\tag{9}$$

The explicit form of F_{va} for a state of angular momentum JM is

$$F_{va}=\sum_{\mu_v\mu_a}\langle j_v\mu_v j_a\mu_a|j_vj_aJM\rangle.\tag{10}$$

In the following, we will have occasion to also use b,c, and d to represent a $1s$ state with magnetic quantum number μ_b, μ_c, and μ_d, and w, x, and y for the same excited state but with magnetic quantum numbers μ_w, μ_x, and μ_y. We note that $2\,^3P_1$ and $2\,^1P_1$ states at low Z will not be well described by this method because they involve strong mixing of states with $v=2p_{1/2}$ and $v=2p_{3/2}$; however, a Green's-function approach does allow treatment of these states [7].

The electron Green's functions can be treated either as a spectral representation or else in terms of solutions to the Dirac equation regular at infinity or the origin. Because in the present calculation we use the former technique, it is convenient to define the frequently encountered object, which we will refer to as the Coulomb matrix element,

$$\begin{aligned}g_{ijkl}(z)\equiv-4\pi\alpha\int d^3r\,d^3r'\,H(\vec{r}-\vec{r}\,',z)\phi_i^\dagger(\vec{r})\\ \times\alpha_\mu\phi_k(\vec{r})\phi_j^\dagger(\vec{r}\,')\alpha^\mu\phi_l(\vec{r}\,').\end{aligned}\tag{11}$$

We note that it is an even function of z and obeys the symmetry relation $g_{ijkl}=g_{jilk}$. We also define for future reference two related forms,

$$\begin{aligned}\tilde{g}_{ijkl}(z)\equiv\alpha\int d^3r\,d^3r'\frac{e^{iz|\vec{r}-\vec{r}\,'|}}{|\vec{r}-\vec{r}\,'|}\\ \times\phi_i^\dagger(\vec{r})\alpha_\mu\phi_k(\vec{r})\phi_j^\dagger(\vec{r}\,')\alpha^\mu\phi_l(\vec{r}\,')\end{aligned}\tag{12}$$

and

$$\begin{aligned}\bar{g}_{ijkl}(z)\equiv\alpha\int d^3r\,d^3r'\frac{\sin(z|\vec{r}-\vec{r}\,'|)}{|\vec{r}-\vec{r}\,'|}\\ \times\phi_i^\dagger(\vec{r})\alpha_\mu\phi_k(\vec{r})\phi_j^\dagger(\vec{r}\,')\alpha^\mu\phi_l(\vec{r}\,').\end{aligned}\tag{13}$$

If we now use

$$\begin{aligned}\langle 0|a_ba_wa_{n_4}^\dagger a_{n_2}^\dagger a_{n_1}a_{n_3}a_v^\dagger a_a^\dagger|0\rangle\\ =(\delta_{n_4w}\delta_{n_2b}-\delta_{n_4b}\delta_{n_2w})(\delta_{n_3v}\delta_{n_1a}-\delta_{n_3a}\delta_{n_1v})\end{aligned}\tag{14}$$

along with the above-noted properties of g_{ijlk}, we find that the fourth-order S-matrix terms we are considering become

$$\begin{aligned}\langle S_\epsilon^{(4)}\rangle_{\mathrm{L}}=F_{va}F_{wb}\int_{-\infty}^{\infty}dq_2\int_{-\infty}^{\infty}dq_1\int_{-\infty}^{\infty}dz_2\int_{-\infty}^{\infty}dz_1\\ \times\sum_{ij}\frac{1}{(E_i-uz_2)(E_j-uz_1)}[g_{bwij}(q_2)g_{ijav}(q_1)\\ \times D_\epsilon(E_a-z_2-q_2)D_\epsilon(E_a-z_2+q_1)\\ \times D_\epsilon(E_v-z_1+q_2)D_\epsilon(E_v-z_1-q_1)-g_{bwij}(q_2)\\ \times g_{ijva}(q_1)D_\epsilon(E_a-z_2-q_2)D_\epsilon(E_v-z_2+q_1)\\ \times D_\epsilon(E_v-z_1+q_2)D_\epsilon(E_a-z_1-q_1)]\end{aligned}\tag{15}$$

and

$$\begin{aligned}\langle S_\epsilon^{(4)}\rangle_{\mathrm{X}}=F_{va}F_{wb}\int_{-\infty}^{\infty}dq_2\int_{-\infty}^{\infty}dq_1\int_{-\infty}^{\infty}dz_2\int_{-\infty}^{\infty}dz_1\\ \times\sum_{ij}\frac{1}{(E_i-uz_2)(E_j-uz_1)}[g_{bjiv}(q_2)g_{iwaj}(q_1)\\ \times D_\epsilon(E_a-z_2-q_2)D_\epsilon(E_a-z_2+q_1)\\ \times D_\epsilon(E_v-z_1+q_1)D_\epsilon(E_v-z_1-q_2)-g_{bjia}(q_2)\\ \times g_{iwvj}(q_1)D_\epsilon(E_a-z_2-q_2)D_\epsilon(E_v-z_2+q_1)\\ \times D_\epsilon(E_v-z_1+q_1)D_\epsilon(E_a-z_1-q_2)].\end{aligned}\tag{16}$$

Here

$$D_\epsilon(x)\equiv\frac{1}{\pi}\frac{\epsilon}{\epsilon^2+x^2} \tag{17}$$

acts like a δ function in the limit $\epsilon\rightarrow 0$; however, it is necessary in general to keep its exact form until it is safe to take that limit. The first and second terms of the above equations will be referred to in the following as the direct (D) and exchange (E) terms, respectively, so that we will be dealing with four terms, the direct and exchange parts of the ladder (LD and LE) and the direct and exchange parts of the crossed ladder (XD and XE).

The fourth-order terms just considered, if treated by themselves, lead to an energy that diverges as $1/\epsilon$. This divergence is canceled by the second term of Eq. (1), which depends on the second-order S matrix,

$$\langle S_\epsilon^{(2)}\rangle_{\mathrm{E}}=-2\pi i F_{va}F_{wb}\int_{-\infty}^{\infty}dq[g_{bwav}(q)D_\epsilon^2(q) -g_{bwva}(q)D_\epsilon^2(q+\delta E)]. \tag{18}$$

The explicit form of this energy shift, which we denote as $\Delta E_{1/\epsilon}$, is

$$\Delta E_{1/\epsilon}=\lim_{\epsilon\rightarrow 0}4i\pi^2\epsilon F_{va}F_{wb}\int_{-\infty}^{\infty}dq_1[g_{bwav}(q_1)D_\epsilon^2(q_1) -g_{bwva}(q_1)D_\epsilon^2(q_1-\delta E)]F_{xc}F_{yd} \times\int_{-\infty}^{\infty}dq_2[g_{dycx}(q_2)D_\epsilon^2(q_2) -g_{dyxc}(q_2)D_\epsilon^2(q_2-\delta E)]. \tag{19}$$

At this point we divide the calculation into two parts. In the first, we restrict the summation over i and j to exclude states in which $E_i+E_j=E_a+E_v$ for the direct and exchange parts of the ladder. In addition, for the direct part of the crossed ladder we exclude the case $E_i=E_a,E_j=E_v$, and for the exchange part of the crossed ladder we exclude the cases $E_i=E_j=E_a$ and $E_i=E_j=E_v$. The excluded states coincide with those considered by Shabaev and Fokeeva [6]. Once these restrictions have been made, the limit $\epsilon\rightarrow 0$ can be taken, and expressions for the associated energy shifts derived.

The excluded states must be treated with greater care. They contain terms proportional to $1/\epsilon$ that cancel exactly against $\Delta E_{1/\epsilon}$. However, after this cancellation a finite part remains, which we refer to as a reference-state contribution. We now present formulas first for the case in which the intermediate states are restricted, and second for the reference-state contributions.

A. Nondegenerate intermediate states

After making the restrictions described above, to derive energy shifts we may expand the photon functions about the dominant contribution to the energy parameter

$$H(\mathbf{x}_2-\mathbf{x}_1,q)=H(\mathbf{x}_2-\mathbf{x}_1,q_0)+O(q-q_0). \tag{20}$$

In Eq. (15), the dominant contributions are in the regions

$$q_2\approx z_1-E_v,\qquad q_1\approx E_v-z_1, \tag{21}$$

in the direct term, and

$$q_2\approx z_1-E_v,\qquad q_1\approx E_a-z_1, \tag{22}$$

in the exchange term. Taking the leading term in the expansion and integrating over q_2 and q_1 yields

$$\langle S_\epsilon^{(4)}\rangle_{\mathrm{L}}=F_{va}F_{wb}\int_{-\infty}^{\infty}dz_2\int_{-\infty}^{\infty}dz_1\sum_{ij}D_{2\epsilon}^2(z_2+z_1-E_v-E_a) \times\frac{g_{bwij}(z_1-E_v)[g_{ijav}(E_v-z_1)-g_{ijva}(E_a-z_1)]}{(E_i-uz_2)(E_j-uz_1)} +O(1). \tag{23}$$

Carrying out the z_2 integration and defining $z=z_1-E_v$, we find

$$E_{\mathrm{L}}^{(4)}=\lim_{\epsilon\rightarrow 0}2i\epsilon\langle S_\epsilon^{(4)}\rangle_{\mathrm{L}} =-\frac{i}{2\pi}F_{va}F_{wb}\int_{-\infty}^{\infty}dz \times\sum_{ij}\frac{g_{bwij}(z)[g_{ijav}(z)-g_{ijva}(z-\delta E)]}{(z+E_a-u^*E_i)(z-E_v+u^*E_j)}. \tag{24}$$

The dominant contributions to the crossed photon diagram in Eq. (16) are in the regions

$$q_2\approx E_v-z_1,\qquad q_1\approx z_1-E_v \tag{25}$$

for the direct term, and

$$q_2\approx E_a-z_1,\qquad q_1\approx z_1-E_v \tag{26}$$

for the exchange term. The leading term yields

$$\langle S_\epsilon^{(4)}\rangle_{\mathrm{X}}=F_{va}F_{wb}\int_{-\infty}^{\infty}dz_2\int_{-\infty}^{\infty}dz_1\sum_{ij}\Bigg[D_{2\epsilon}^2(z_2-z_1+\delta E) \times\frac{g_{bwiv}(E_v-z_1)g_{iwaj}(z_1-E_v)}{(E_i-uz_2)(E_j-uz_1)}-D_{2\epsilon}^2(z_2-z_1) \times\frac{g_{bjia}(E_v-z_1)g_{ivwj}(z_1-E_v)}{(E_i-uz_2)(E_j-uz_1)}\Bigg]+O(1) \tag{27}$$

and the same kind of manipulations as applied to the ladder lead to

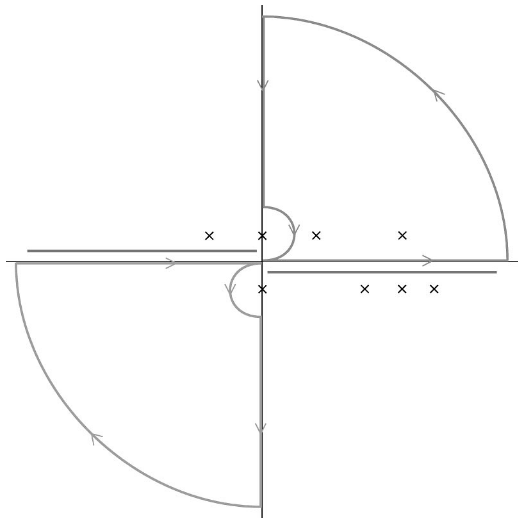

FIG. 1. Contours used for the evaluation of LD.

$$E_{\rm X}^{(4)}=\lim_{\epsilon\to 0}\ 2i\epsilon\langle S_\epsilon^{(4)}\rangle_{\rm X}$$

$$=\frac{i}{2\pi}F_{va}F_{wb}\int_{-\infty}^{\infty}dz\sum_{ij}\ \frac{g_{bjiv}(z)g_{iwaj}(z)}{(z+E_a-u^*E_i)(z+E_v-u^*E_j)}$$

$$-\frac{i}{2\pi}F_{va}F_{wb}\int_{-\infty}^{\infty}dz$$

$$\times\sum_{ij}\ \frac{g_{bjia}(z)g_{iwvj}(z-\delta E)}{(z+E_a-u^*E_i)(z+E_a-u^*E_j)}. \qquad (28)$$

Equations (24) and (28) are the basic formulas of this section.

Were it not for the z dependence of the g factors in these formulas, which is associated with cuts in the complex plane, one could directly evaluate them using Cauchy's theorem. In fact, if the Coulomb gauge is used, this approach can be applied to the Coulomb photon part of the calculation, and expressions closely related to many-body perturbation theory result [8]. However, for an exact calculation in the Feynman gauge, we follow the treatment of Ref. [2] and carry out a Wick rotation. While this was straightforward for the ground-state case, for excited states the poles and cuts associated with the electron and photon propagators create significant complications. Each of the four terms (LD, LE, XD, and XE) requires an individual treatment, which we now present.

1. Ladder direct

The poles and cuts for the direct part of the ladder are shown in Fig. 1. Poles associated with negative energy states are off scale in the second and fourth quadrants, and do not play a role in the Wick rotation. The case $i=a$ leads to a pole just below the origin that is avoided by the semicircle in quadrant III, and the case $j=v$ leads to a pole just above the origin that is avoided by the semicircle in quadrant I. In addition, a set of poles associated with more deeply bound states lies above the positive real axis, and is encircled by the contour in quadrant I. The number of these poles varies depending on which state is being considered. While the most deeply bound $j=a$ state is always encircled, the number of other contributing states ranges between zero and two, with the most complex case being the $2\,^3P_2$ state, in which both $j=2s_{1/2}$ and $j=2p_{1/2}$ contribute. We denote these states with the index j_p. Applying Cauchy's theorem to the contours in quadrants I and III and setting $k_0=i\omega$ to account for the integrations along the complex axis then allows the determination

$$E_{\rm LD}^{(4)}=-\frac{1}{\pi}F_{va}F_{wb}\int_0^{\infty}d\omega\sum_{ij}\ g_{bwij}(i\omega)g_{ijav}(i\omega)$$

$$\times\frac{(E_i-E_a)(E_j-E_v)+\omega^2}{[(E_i-E_a)^2+\omega^2][(E_j-E_v)^2+\omega^2]}-\frac{1}{2}F_{va}F_{wb}$$

$$\times\sum_{cj}^{E_j\neq E_v}\frac{g_{bwcj}(0)g_{cjav}(0)}{E_j-E_v}-F_{va}F_{wb}$$

$$\times\sum_{ij_p}\frac{g_{bwij_p}(E_v-E_{j_p})g_{ij_pav}(E_v-E_{j_p})}{E_i+E_{j_p}-E_v-E_a}A_{j_p}, \qquad (29)$$

where the factor A_{j_p} is 1/2 when $j_p=v$, and unity otherwise.

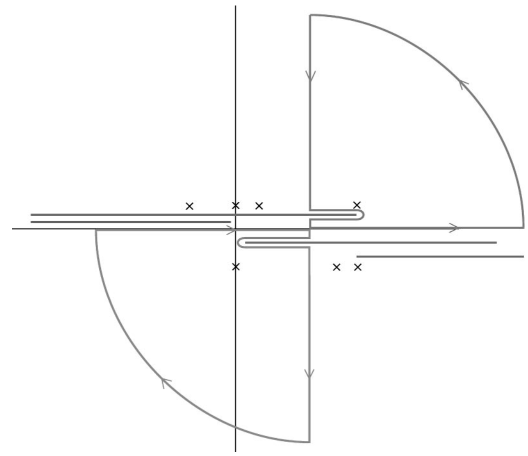

FIG. 2. Contours used for the evaluation of LE.

2. Ladder exchange

While the location of the poles is the same for LE as for LD, one photon propagator has argument $z-\delta E$, which extends a cut into the first quadrant, as shown in Fig. 2. We choose to Wick rotate to $z=\beta\delta E+i\omega$, with β a number between 0 and 1 chosen so that the contours encircle only a single pole each. The value $\beta=0.5$ was usually used, with occasionally different values used to test the coding: when β is changed, both the integration parallel to the imaginary axis and the terms that wrap around the two cuts change, but the sum has to remain unchanged. The sign of the exponent in one of the photon propagators is different above and below a cut, which leads to the modified Coulomb matrix element $\overline{g}_{ijkl}(z)$ defined in Eq. (13). We find

$$E_{\rm LE}^{(4)}=\frac{1}{\pi}F_{va}F_{wb}\ {\rm Re}\int_0^\infty d\omega \times\sum_{ij}\frac{g_{bwij}(\beta\delta E+i\omega)g_{ijva}[(\beta-1)\delta E+i\omega]}{(E_i-E_a-\beta\delta E-i\omega)(E_j-E_v+\beta\delta E+i\omega)} +F_{va}F_{wb}\sum_{cj}^{E_j\neq E_v}\frac{g_{bwcj}(0)g_{cjva}(\delta E)}{E_j-E_v}+F_{va}F_{wb} \times\sum_{ic}^{E_i\neq E_v}\frac{g_{bwic}(\delta E)g_{icva}(0)}{E_i-E_v}-\frac{1}{\pi}F_{va}F_{wb}\sum_{ij}\int_0^{\beta\delta E}dz \times\frac{\overline{g}_{bwij}(z)g_{ijva}[-(z-\delta E)]}{(z+E_a-u^*E_i)(z-E_v+u^*E_j)}+\frac{1}{\pi}F_{va}F_{wb} \times\sum_{ij}\int_{\beta\delta E}^{\delta E}dz\frac{g_{bwij}(z)\overline{g}_{ijva}(z-\delta E)}{(z+E_a-u^*E_i)(z-E_v+u^*E_j)}. \tag{30}$$

We note two features of the cut terms. The first is that the presence of the sin functions leads to additional convergence at the end of the cuts, which controls singularities associated with poles at the end. Second, the infinitesimal imaginary terms $i\delta$ in the denominators have been retained, because there can be poles along the path of the line integral. As with the direct part of the ladder, these poles occur if there are $n=2$ states more deeply bound than the state v. When this situation is encountered, we use the standard identity

$$\frac{1}{z-z_0-i\delta}=PP\frac{1}{z-z_0}+i\pi\delta(z-z_0). \tag{31}$$

We thus can put $\delta=0$ in the cut terms in Eq. (30) as long as we carry out the integrals as principal parts. However, the δ-function term leads to the additional contribution

$$\Delta E_{\rm LE}({\rm extra}) =-iF_{va}F_{wb}\sum_{ij_b}\frac{\overline{g}_{bwij_b}(E_v-E_{j_b})g_{ij_bva}(E_a-E_{j_b})}{(E_v+E_a-E_i-E_{j_b})} +iF_{va}F_{wb}\sum_{i_bj}\frac{g_{bwi_bj}(E_{i_b}-E_a)\overline{g}_{i_bjva}(E_{i_b}-E_v)}{(E_v+E_a-E_{i_b}-E_j)}, \tag{32}$$

where i_b and j_b in this case range over any $n=2$ states more deeply bound than v. It is noteworthy that these contributions would affect only the decay rate if the g and $\overline{g}$ factors were real, but as they are in general complex, a finite, though extremely small, energy shift is present.

3. Crossed ladder direct

Figure 3 shows the poles and cuts that affect XD: in this case the pole structure affects only the contour in the third quadrant. However, the pole just below the origin can come either from the case $i=a$ or $j=v$, so two contributions result. We recall that the case $i=v, j=a$, which has a double pole, is treated separately. An analysis similar to that of the LD gives

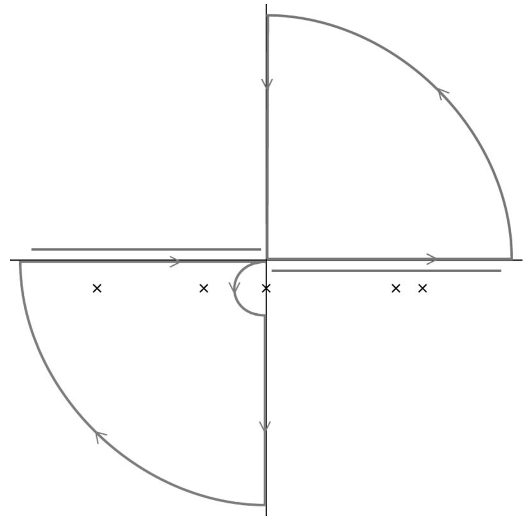

FIG. 3. Contours used for the evaluation of XD.

$$E_{\rm XD}^{(4)}=-\frac{1}{\pi}F_{va}F_{wb}\int_0^\infty d\omega\sum_{ij}g_{bjiv}(i\omega)g_{iwaj}(i\omega) \times\frac{(E_i-E_a)(E_j-E_v)-\omega^2}{[(E_i-E_a)^2+\omega^2][(E_j-E_v)^2+\omega^2]}-\frac{1}{2}F_{va}F_{wb} \times\sum_{cj}^{E_j\neq E_v}\frac{g_{bjcv}(0)g_{cwaj}(0)}{E_j-E_v}-F_{va}F_{wb} \times\sum_{ij_b}{}'\frac{g_{bj_biv}(E_{j_b}-E_v)g_{iwaj_b}(E_{j_b}-E_v)}{E_i-E_{j_b}+E_v-E_a}A_{j_b}. \tag{33}$$

4. Crossed ladder exchange

The pole and cut structure of XE is shown in Fig. 4. As with LE, the displacement of the photon cuts requires con-

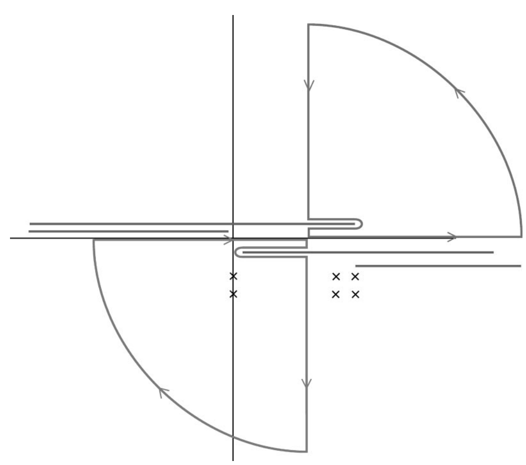

FIG. 4. Contours used for the evaluation of XE.

tours that wrap around them as indicated in the figure. Applying Cauchy's theorem to the two contours allows the determination

$$E_{\rm XE}^{(4)}=\frac{1}{\pi}F_{va}F_{wb}\ {\rm Re}\int_0^\infty d\omega \times\sum_{ij}\frac{g_{bjia}(\beta\delta E+i\omega)g_{iwvj}[(\beta-1)\delta E+i\omega]}{(E_i-E_a-\beta\delta E-i\omega)(E_j-E_a-\beta\delta E-i\omega)} +F_{va}F_{wb}\sum_{cj}^{E_j\neq E_a}\frac{g_{bjca}(0)g_{cwvj}(-\delta E)}{E_j-E_a}+F_{va}F_{wb} \times\sum_{ic}^{E_i\neq E_a}\frac{g_{bcia}(0)g_{iwvc}(-\delta E)}{E_i-E_a}-\frac{1}{\pi}F_{va}F_{wb} \times\sum_{ij}\int_{\beta\delta E}^{\delta E}dz\frac{g_{bjia}(z)\overline{g}_{iwvj}(z-\delta E)}{(z+E_a-u^*E_i)(z+E_a-u^*E_j)} +\frac{1}{\pi}F_{va}F_{wb}\sum_{ij}\int_0^{\beta\delta E}dz \times\frac{\overline{g}_{bjia}(z)g_{iwvj}[-(z-\delta E)]}{(z+E_a-u^*E_i)(z+E_a-u^*E_j)}. \tag{34}$$

As with LE, the integrations in the cut terms can be understood as principal value integrations, but an extra term is generated,

$$\Delta E_{\rm XE}({\rm extra}) =iF_{va}F_{wb}\sum_{ij_b}\frac{g_{bj_bia}(E_{j_b}-E_a)\overline{g}_{iwvj_b}(E_{j_b}-E_v)}{E_{j_b}-E_i} +iF_{va}F_{wb}\sum_{i_bj}\frac{g_{bji_ba}(E_{i_b}-E_a)\overline{g}_{i_bwvj}(E_{i_b}-E_v)}{E_{i_b}-E_j}. \tag{35}$$

As with the LE case, this extra term is very small numerically. An interesting feature of this term is the fact that even with the restriction on the state that we have made, the denominator can vanish when the valence state is not the most deeply bound $n=2$ state. In this case, the divergence indicates a more careful analysis is needed. In principle, to define the integral it is necessary to deform the contour in a semicircle around the double pole. However, in practice it is possible to obtain the correct answer by symmetrically integrating with two different numbers of Gaussian points and taking a certain linear combination. This effect is numerically insignificant except at very high Z.

B. Reference-state contributions

When it is not permissible to approximate the arguments of the photon propagators as done above, a different procedure must be followed. In sensitive cases we first carry out the z_1 and z_2 integrals. As in the ground-state case [2], it is convenient to define the integral

$$f_\epsilon(q_2,q_1)\equiv\pi^2\int_{-\infty}^\infty dz\frac{1}{E-uz}D_\epsilon(E-z-q_2)D_\epsilon(E-z+q_1) =-\frac{\pi^2}{2}D_{2\epsilon}(q_2+q_1)\frac{q_2-q_1-4i\epsilon}{(q_2-i\epsilon)(q_1+i\epsilon)}. \tag{36}$$

In terms of this function, the energy shift associated with Eq. (15) can be written as

$$\Delta E_{\rm L}=\frac{2i\epsilon}{\pi^4}\int_{-\infty}^\infty dq_2\int_{-\infty}^\infty dq_1\,F_{va}F_{wb}\sum_{ij}[g_{bwij}(q_2) \times g_{ijav}(q_1)f_\epsilon(q_2+E_i-E_a,q_1+E_a-E_i) \times f_\epsilon(q_1+E_j-E_v,q_2+E_v-E_j)-g_{bwij}(q_2) \times g_{ijva}(q_1)f_\epsilon(q_2+E_i-E_a,q_1+E_v-E_i) \times f_\epsilon(q_1+E_j-E_a,q_2+E_v-E_j)] \tag{37}$$

and the energy shift associated with Eq. (16) as

$$\Delta E_{\rm X}=\frac{2i\epsilon}{\pi^4}\int_{-\infty}^\infty dq_2\int_{-\infty}^\infty dq_1F_{va}F_{wb}\sum_{ij}[g_{bjiv}(q_2)g_{iwaj}(q_1) \times f_\epsilon(q_2+E_i-E_a,q_1+E_a-E_i) \times f_\epsilon(q_2+E_j-E_v,q_1+E_v-E_j)-g_{bjia}(q_2)g_{iwvj}(q_1) \times f_\epsilon(q_2+E_i-E_a,q_1+E_v-E_i) \times f_\epsilon(q_2+E_j-E_a,q_1+E_v-E_j)]. \tag{38}$$

Equation (37) contains a term that diverges as $1/\epsilon$, which cancels with Eq. (19). In order to isolate it we use the identity

$$f_\epsilon(q_2,q_1)f_\epsilon(q_1,q_2)=\frac{1}{2}[f_\epsilon(q_2,q_1)+f_\epsilon(q_1,q_2)]^2 -\frac{1}{2}[f_\epsilon^2(q_2,q_1)+f_\epsilon^2(q_1,q_2)] =-2\pi^6D_\epsilon^2(q_2)D_\epsilon^2(q_1) -\frac{1}{2}[f_\epsilon^2(q_2,q_1)+f_\epsilon^2(q_1,q_2)]. \tag{39}$$

We now insert the first part of this identity into Eq. (37) for the cases $i=a,j=v$ and $i=v,j=a$, and find

$$\Delta E_{\rm L}\left(\frac{1}{\epsilon}\right)=-4\pi^2i\epsilon\sum_{cx}F_{va}F_{wb}\int_{-\infty}^\infty dq_2\int_{-\infty}^\infty dq_1 \times[g_{bwcx}(q_2)g_{cxav}(q_1)D_\epsilon^2(q_2)D_\epsilon^2(q_2) +g_{bwxc}(q_2)g_{xcav}(q_1)D_\epsilon^2(q_2+\delta E)D_\epsilon^2(q_1-\delta E) -g_{bwcx}(q_2)g_{cxva}(q_1)D_\epsilon^2(q_2)D_\epsilon^2(q_1+\delta E) -g_{bwxc}(q_2)g_{xcva}(q_1)D_\epsilon^2(q_2+\delta E)D_\epsilon^2(q_1)]. \tag{40}$$

The integrals over q_1 and q_2 are identical to $\Delta E_{1/\epsilon}$, given in Eq. (19), but the indices of the g factors are not. However, if we use the identity

$$\sum_{JM} \langle j_v \mu_x j_a \mu_c | JM \rangle \langle JM | j_v \mu_y j_a \mu_d \rangle = \delta_{\mu_x \mu_y} \delta_{\mu_c \mu_d}, \tag{41}$$

we can rewrite

$$\begin{aligned} \Delta E_{\rm L}\left(\frac{1}{\epsilon}\right) = & -4\pi^2 i \epsilon \sum_{cxdy} F_{va} F_{wb} \sum_{J'M'} \langle j_v \mu_x j_a \mu_c | J'M' \rangle \\ & \times \langle J'M' | j_v \mu_y j_a \mu_d \rangle \int_{-\infty}^{\infty} dq_2 \int_{-\infty}^{\infty} dq_1 \\ & \times [g_{bwcx}(q_2) g_{dyav}(q_1) D_\epsilon^2(q_2) D_\epsilon^2(q_1) \\ & + g_{bwxc}(q_2) g_{ydav}(q1) D_\epsilon^2(q_2+\delta E) D_\epsilon^2(q_1-\delta E) \\ & - g_{bwcx}(q_2) g_{dyva}(q_1) D_\epsilon^2(q_2) D_\epsilon^2(q_1+\delta E) \\ & - g_{bwxc}(q_2) g_{ydva}(q_1) D_\epsilon^2(q_2+\delta E) D_\epsilon^2(q_1)]. \end{aligned} \tag{42}$$

Because the exchange of a photon is a scalar operator that cannot change angular momentum, $J'M'$ will be forced to equal JM, and the above becomes

$$\begin{aligned} \Delta E_{\rm L}\left(\frac{1}{\epsilon}\right) = & -4\pi^2 i \epsilon F_{va} F_{xc} F_{wb} F_{yd} \int_{-\infty}^{\infty} dq_2 \int_{-\infty}^{\infty} dq_1 \\ & \times [g_{bwcx}(q_2) g_{dyav}(q_1) D_\epsilon^2(q_2) D_\epsilon^2(q_1) \\ & + g_{bwxc}(q_2) g_{ydav}(q_1) D_\epsilon^2(q_2+\delta E) D_\epsilon^2(q_1-\delta E) \\ & - g_{bwcx}(q_2) g_{dyva}(q_1) D_\epsilon^2(q_2) D_\epsilon^2(q_1+\delta E) \\ & - g_{bwxc}(q_2) g_{ydva}(q_1) D_\epsilon^2(q_2+\delta E) D_\epsilon^2(q_1)], \end{aligned} \tag{43}$$

which can be seen to cancel $\Delta E_{1/\epsilon}$ after rearrangement of dummy indices and use of symmetry. It is important to note that no approximations have been made in manifesting this cancellation, since otherwise the presence of the factor of $1/\epsilon$ could lead to a residual finite term.

After isolating and canceling the divergent terms, finite terms, which we will refer to as reference-state contributions, remain. The LD terms in the case $i=a, j=v$ give

$$\begin{aligned} \Delta E_{\rm LD}^{\rm ref}(av) = & -\frac{i\epsilon}{\pi^4} F_{va} F_{wb} \int_{-\infty}^{\infty} dq_2 \int_{-\infty}^{\infty} dq_1 \sum_{cx} g_{bwcx}(q_2) \\ & \times g_{cxav}(q_1)[f_\epsilon(q_2,q_1)^2 + f_\epsilon(q_1,q_2)^2]. \end{aligned} \tag{44}$$

Because the f functions emphasize the region $q_1+q_2=0$, we can approximate $g_{bwcx}(q_2) = g_{bwcx}(-q_1)$ in the above, which allows the integral over q_2 to be carried out, with the result

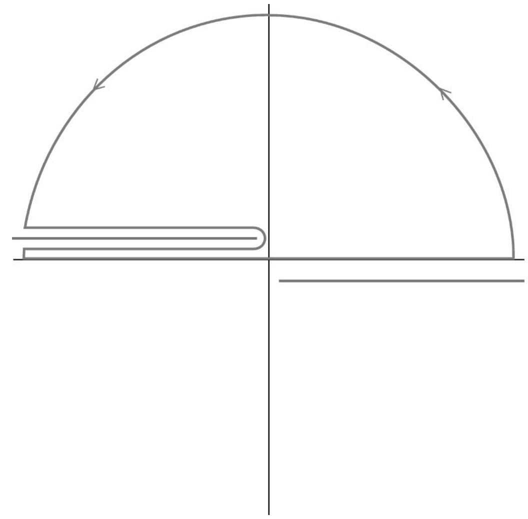

FIG. 5. Contours used for the evaluation of LD and XD reference-state terms.

$$\begin{aligned} \Delta E_{\rm LD}^{\rm ref}(av) = & -\frac{i}{4\pi} F_{va} F_{wb} \int_{-\infty}^{\infty} dq \sum_{cx} g_{bwcx}(q) \\ & \times g_{cxav}(q) D(q), \end{aligned} \tag{45}$$

where

$$D(q) \equiv \frac{q+5i\epsilon}{(q+i\epsilon)^2(q+3i\epsilon)} + \frac{q-5i\epsilon}{(q-i\epsilon)^2(q-3i\epsilon)}. \tag{46}$$

The first term of $D(q)$ has a pole and a double pole in quadrant IV, and the second has a pole and a double pole in quadrant I. The position of these poles will be important in the following, where we use Cauchy's theorem to analyze the q integrations, but once that is done we will replace $D(q)$ with its $\epsilon \to 0$ limit, $2/q^2$. Individual terms obtained with this procedure will have logarithmic singularities, which, however, cancel in the sum, as will be discussed below.

The contour used for the evaluation of $\Delta E_{\rm LD}^{\rm ref}(av)$ is shown in Fig. 5, and leads to

$$\begin{aligned} \Delta E_{\rm LD}^{\rm ref}(av) = & \frac{i}{2\pi} F_{va} F_{wb} \int_{-\infty}^{0} \frac{dq}{q^2} \sum_{cx} [\tilde{g}_{bwcx}(q) \tilde{g}_{cxav}(q) \\ & - \tilde{g}_{bwcx}(-q) \tilde{g}_{cxav}(-q)]. \end{aligned} \tag{47}$$

In the above, Fig. 5 was actually applied only to the first term of $D(q)$, as the second term would involve enclosed poles: however, symmetry arguments show that the second term of $D(q)$ in fact gives the same contribution. The apparent linear divergence of this integral at $q=0$ is softened to a logarithmic divergence because the combination of g factors vanishes as q in that limit. The remaining divergence cancels against the XD reference-state term treated below.

The LE term for the $i,j=a,v$ case is

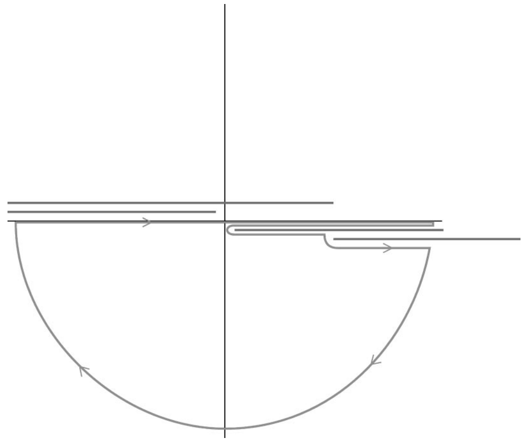

FIG. 6. Contours used for the evaluation of LE(av) and XE(aa) reference-state terms.

$$\Delta E^{\rm ref}_{\rm LE}(av) = \frac{i\epsilon}{\pi^4} F_{va}F_{wb}\int_{-\infty}^{\infty}dq_2\int_{-\infty}^{\infty}dq_1\sum_{cx} g_{bwcx}(q_2) \times g_{cxva}(q_1)[f_\epsilon(q_2,q_1+\delta E)^2 + f_\epsilon(q_1+\delta E,q_2)^2]. \quad (48)$$

In this case we approximate $g_{bwcx}(q_2)=g_{bwcx}(-q_1-\delta E)$, and after carrying out the integral over q_2 we find

$$\Delta E^{\rm ref}_{\rm LE}(av) = \frac{i}{4\pi} F_{va}F_{wb}\int_{-\infty}^{\infty}dq\sum_{cx} g_{bwcx}(q) g_{cxva}(\overline{q}) D(q), \quad (49)$$

where $\overline{q}\equiv q-\delta E$. The contour we use in this case is shown in Fig. 6. The first term of $D(q)$ has a double pole inside the contour which leads to an additional derivative term, and the total contribution is

$$\Delta E^{\rm ref}_{\rm LE}(av) = -\frac{1}{\pi} F_{va}F_{wb}\int_0^{\delta E}\frac{dq}{q^2}\sum_{cx} \overline{g}_{bwcx}(q)\tilde{g}_{cxva}(-\overline{q}) + \frac{i}{2\pi}F_{va}F_{wb}\int_{\delta E}^{\infty}\frac{dq}{q^2}\sum_{cx}[\tilde{g}_{bwcx}(q)\tilde{g}_{cxva}(\overline{q}) - \tilde{g}_{bwcx}(-q)\tilde{g}_{cxva}(-\overline{q})] + \frac{1}{2}F_{va}F_{wb}\sum_{cx} g_{bwcx}(0)g'_{cxva}(-\delta E). \quad (50)$$

We have used the fact that $g'_{ijkl}(0)=0$ in the above. The first term has a logarithmic singularity at $q=0$ that cancels with the part of XE associated with the exclusion of $i=a,j=a$.

We now consider the ladder direct term when $i=v,j=a$. After removing the divergent term, there remains

$$\Delta E^{\rm ref}_{\rm LD}(va) = -\frac{i\epsilon}{\pi^4} F_{va}F_{wb}\int_{-\infty}^{\infty}dq_2\int_{-\infty}^{\infty}dq_1\sum_{xc} g_{bwxc}(q_2) \times g_{xcav}(q_1)[f_\epsilon(q_2+\delta E,q_1-\delta E)^2 + f_\epsilon(q_1-\delta E,q_2+\delta E)^2]. \quad (51)$$

Approximating $g_{bwxc}(q_2)=g_{bwxc}(-q_1)$ and carrying out the q_2 integration gives

$$\Delta E^{\rm ref}_{\rm LD}(va) = -\frac{i}{4\pi} F_{va}F_{wb}\int_{-\infty}^{\infty}dq\sum_{cx} g_{bwxc}(q) \times g_{xcav}(q)D(\overline{q}). \quad (52)$$

We again use the contour shown in Fig. 5 for the evaluation of this term. One term of $D(\overline{q})$ again leads to a derivative term, with a total result of

$$\Delta E^{\rm ref}_{\rm LD}(va) = \frac{1}{2}F_{va}F_{wb}\sum_{xc}[g'_{bwxc}(\delta E)g_{xcav}(\delta E) + g_{bwxc}(\delta E)g'_{xcav}(\delta E)] + \frac{i}{2\pi}F_{va}F_{wb} \times \sum_{xc}\int_{-\infty}^{0}\frac{dq}{\overline{q}^2}[\tilde{g}_{bwxc}(q)\tilde{g}_{xcav}(q) - \tilde{g}_{bwxc}(-q)\tilde{g}_{xcav}(-q)]. \quad (53)$$

The analysis of LE for the case $i,j=v,a$ gives

$$\Delta E^{\rm ref}_{\rm LE}(va) = \frac{i\epsilon}{\pi^4} F_{va}F_{wb}\int_{-\infty}^{\infty}dq_2\int_{-\infty}^{\infty}dq_1\sum_{xc} g_{bwxc}(q_2) \times g_{xcva}(q_1)[f_\epsilon(q_2+\delta E,q_1)^2 + f_\epsilon(q_1,q_2+\delta E)^2], \quad (54)$$

which leads to

$$\Delta E^{\rm ref}_{\rm LE}(va) = \frac{i}{4\pi} F_{va}F_{wb}\int_{-\infty}^{\infty}dq\sum_{cx} g_{bwxc}(q) g_{xcva}(\overline{q}) D(\overline{q}). \quad (55)$$

Using the contour of Fig. 7 then leads to

$$\Delta E^{\rm ref}_{\rm LE}(va) = -\frac{1}{2}F_{va}F_{wb}\sum_{xc} g'_{bwxc}(\delta E)g_{xcva}(0) + \frac{1}{\pi}F_{av}F_{bw}\sum_{xc}\int_0^{\delta E}\frac{dq}{\overline{q}^2}\tilde{g}_{bwxc}(q)\overline{g}_{xcva}(\overline{q}) - \frac{i}{2\pi}F_{va}F_{wb}\int_{-\infty}^{0}\frac{dq}{\overline{q}^2}[\tilde{g}_{bwxc}(q)\tilde{g}_{xcva}(\overline{q}) - \tilde{g}_{bwxc}(-q)\tilde{g}_{xcva}(-\overline{q})]. \quad (56)$$

The second term has a logarithmic singularity at $q=\delta E$ which cancels with the part of XE associated with $i=v,j=v$.

Turning now to XD, we recall that only $i=a,j=v$ was restricted, which leads, after an analysis similar to that applied to LD, to the contribution

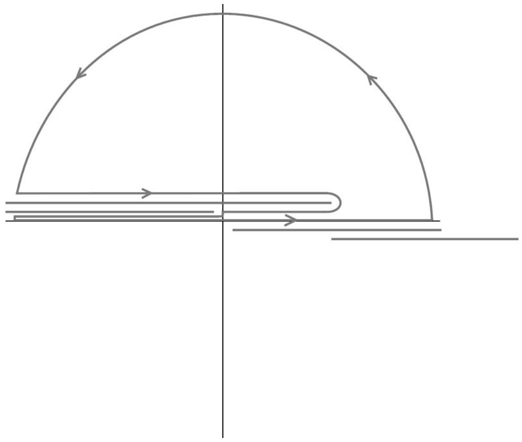

FIG. 7. Contours used for the evaluation of LE(va) and XE(vv) reference-state terms.

$$\Delta E^{\rm ref}_{\rm XD}=\frac{i}{2\pi}F_{va}F_{wb}\sum_{cx}\int_{-\infty}^{\infty}dq\; g_{bxcv}(q)\times g_{cwax}(q)\frac{q+5i\epsilon}{(q+i\epsilon)^2(q+3i\epsilon)}, \tag{57}$$

which when evaluated with the contour of Fig. 5 becomes

$$\Delta E^{\rm ref}_{\rm XD}(av)=-\frac{i}{2\pi}F_{va}F_{wb}\int_{-\infty}^{0}\frac{dq}{q^2}\sum_{cx}[\tilde g_{bxcv}(q)\tilde g_{cwax}(q)-\tilde g_{bxcv}(-q)\tilde g_{cwax}(-q)]. \tag{58}$$

We note the close similarity to $\Delta E_{\rm LD}(av)$. However, while the two terms are of a form to cancel, the indices on the Coulomb matrix elements are different, and in fact the cancellation is not exact. The divergences present in the individual terms are, however, not present in their sum.

Finally, XE has reference-state contributions from a set of states of equal energy. When the states are the ground state, we have

$$\Delta E^{\rm ref}_{\rm XE}(aa)=-\frac{i}{2\pi}F_{va}F_{wb}\sum_{cd}\int_{-\infty}^{\infty}dq\; g_{bdca}(q)\times g_{cwvd}(q-\delta E)\frac{q+5i\epsilon}{(q+i\epsilon)^2(q+3i\epsilon)} \tag{59}$$

and when they are $n=2$ states, we have

$$\Delta E^{\rm ref}_{\rm XE}(xx)=-\frac{i}{2\pi}F_{va}F_{wb}\sum_{xy}\int_{-\infty}^{\infty}dq\; g_{byxa}(q)\times g_{xwvy}(q-\delta E)\frac{\bar q+5i\epsilon}{(\bar q+i\epsilon)^2(\bar q+3i\epsilon)}. \tag{60}$$

In the former case we use the contour of Fig. 6 to find

$$\Delta E^{\rm ref}_{\rm XE}(aa)=-F_{va}F_{wb}\sum_{cd}g_{bdca}(0)g'_{cwvd}(-\delta E)+\frac{1}{\pi}F_{va}F_{wb}\sum_{cd}\int_0^{\delta E}dq\;\overline{g}_{bdca}(q)\tilde g_{cwvd}(-\bar q)\times\frac{q+5i\epsilon}{(q+i\epsilon)^2(q+3i\epsilon)}-\frac{i}{2\pi}F_{va}F_{wb}\times\sum_{cd}\int_{\delta E}^{\infty}\frac{dq}{q^2}[\tilde g_{bdca}(q)\tilde g_{cwvd}(\bar q)-\tilde g_{bdca}(-q)\tilde g_{cwvd}(-\bar q)]. \tag{61}$$

In the latter, use of the contour of Fig. 7 gives

$$\Delta E^{\rm ref}_{\rm XE}(vv)=-\frac{1}{\pi}F_{va}F_{wb}\sum_{xy}\int_0^{\delta E}dq\;\tilde g_{byxa}(q)\overline{g}_{xwvy}(\bar q)\times\frac{\bar q+5i\epsilon}{(\bar q+i\epsilon)^2(\bar q+3i\epsilon)}+\frac{i}{2\pi}F_{va}F_{wb}\times\sum_{xy}\int_{-\infty}^{0}\frac{dq}{\bar q^2}[\tilde g_{byxa}(q)\tilde g_{xwvy}(\bar q)-\tilde g_{byxa}(-q)\tilde g_{xwvy}(-\bar q)]. \tag{62}$$

The logarithmic singularities at $q=0$ and $q=\delta E$ cancel against similar terms in the LE reference-state term.

The reference-state terms were grouped into seven classes, referred to in the following as R_0-R_6. These are finite rearrangements of the expressions for $\Delta E^{\rm ref}_{\rm LD}(av)$ [Eq. (46)], $\Delta E^{\rm ref}_{\rm LD}(va)$ [Eq. (52)], $\Delta E^{\rm ref}_{\rm LE}(av)$ [Eq. (49)], $\Delta E^{\rm ref}_{\rm LE}(va)$ [Eq. (55)], $\Delta E^{\rm ref}_{\rm XD}(av)$ [Eq. (57)], $\Delta E^{\rm ref}_{\rm XE}(aa)$ [Eq. (60)], and $\Delta E^{\rm ref}_{\rm XE}(vv)$ [Eq. (61)]. Specifically, R_0 is defined to be the sum of $\Delta E^{\rm ref}_{\rm LD}(av)$ and $\Delta E^{\rm ref}_{\rm XD}(av)$. R_1 is the sum of the first term of $\Delta E^{\rm ref}_{\rm LE}(av)$, the second term of $\Delta E^{\rm ref}_{\rm LE}(va)$, the second term of $\Delta E^{\rm ref}_{\rm XE}(aa)$, and the first term of $\Delta E^{\rm ref}_{\rm XE}(vv)$. R_2 is defined as the sum of the second term of $\Delta E^{\rm ref}_{\rm LE}(av)$ and the third term of $\Delta E^{\rm ref}_{\rm LE}(va)$. R_3 is the second part of $\Delta E^{\rm ref}_{\rm LD}(va)$, R_4 the third part of $\Delta E^{\rm ref}_{\rm XE}(aa)$, and R_5 the second part of $\Delta E^{\rm ref}_{\rm XE}(vv)$. Finally, R_6 is the sum of the derivative terms appearing in $\Delta E^{\rm ref}_{\rm LE}(av)$, $\Delta E^{\rm ref}_{\rm LD}(va)$, and $\Delta E^{\rm ref}_{\rm XE}(aa)$.

III. NUMERICAL RESULTS AND COMPARISON WITH MANY-BODY PERTURBATION THEORY

In this section we numerically evaluate the formulas derived above for a set of heliumlike ions. The basic numerical technique is that of finite basis sets [9]. A basis set with 50 positive and 50 negative energy states was formed in a cavity of radius $R_m=100/Z$ a.u. Larger and smaller basis sets were used to ensure that basis-set dependences were negligible. The integrations parallel to the imaginary axis were carried out with Gaussian methods. Particular care is required for the direct diagrams at low values of the integration variable ω because of the structure arising from nearby poles. In par-

TABLE I. Summary of $Z=30$ calculation.

	$2\,^3S_1$	$2\,^3P_0$	$2\,^3P_2$
$l=0$	0.010 446 24	0.008 139 42	0.008 228 57
$l=1$	−0.000 627 05	−0.005 028 20	−0.002 299 07
$l=2$	−0.000 156 59	0.000 291 40	0.001 009 77
$l=3$	−0.000 026 69	0.000 007 99	0.000 041 54
$l=4$	−0.000 006 95	−0.000 005 52	0.000 007 89
$l=5$	−0.000 002 37	−0.000 004 48	0.000 001 99
$l=6$	−0.000 000 98	−0.000 002 98	0.000 000 61
$l=7$	−0.000 000 47	−0.000 001 99	0.000 000 21
$l=8$	−0.000 000 25	−0.000 001 36	0.000 000 07
$l=9$	−0.000 000 14	−0.000 000 96	0.000 000 02
$l=10$	−0.000 000 09	−0.000 000 70	0.000 000 00
$l=0-10$	0.009 624 67	0.003 392 61	0.006 991 60
poles	−0.061 032 74	−0.093 800 18	−0.084 302 16
cuts	−0.000 008 48	0.000 008 65	0.000 009 63
reference states	0.001 866 47	0.001 791 90	0.002 025 81
total	−0.049 550 08	−0.088 607 03	−0.075 275 12

ticular, the $2s_{1/2}$ and $2p_{1/2}$ states are split only by finite nuclear size effects, and this splitting is quite small at the lower values of Z used here.

We give the detailed breakdown of the calculation for heliumlike zinc, $Z=30$. Using $c=4.4454$ fm, the energies of the $2s_{1/2}$, $2p_{1/2}$, and $2p_{3/2}$ states are $-114.228\,104$ a.u., $-114.228\,639$ a.u., and $-112.839\,015$ a.u., respectively, which illustrates the near-degeneracy mentioned above. In Table I, we present a summary of the calculation for the three states $2\,^3S_1$, $2\,^3P_0$, and $2\,^3P_2$: as mentioned earlier, the presence of mixing for the $2\,^3P_1$ state requires a modification of the present method [10]. The parameter β is chosen to be 1/2.

The terms in the exchange graphs in which integrals along the cut are involved are seen to be relatively small, and are in fact pure QED effects, as they vanish in the absence of retardation.

Some of the reference-state terms are individually divergent, though these divergences cancel pairwise. These inte-

TABLE II. Breakdown of reference-state contributions at $Z=30$.

	$2\,^3S_1$	$2\,^3P_0$	$2\,^3P_2$
R_0	−0.000 000 07	0.000 000 59	−0.000 000 09
R_1	0.000 000 72	0.000 000 13	0.000 000 21
R_2	−0.003 908 49	−0.002 886 97	−0.003 086 88
R_3	0.000 060 88	0.000 033 69	0.000 040 02
R_4	0.003 858 75	0.002 578 20	0.002 809 64
R_5	0.001 479 21	0.001 129 84	0.001 246 52
R_{6a}	−0.000 182 61	−0.000 594 65	−0.000 612 12
R_{6b}	0.000 019 27	0.000 034 76	0.000 040 31
R_{6c}	0.000 538 81	0.001 496 31	0.001 588 21
total	0.001 866 47	0.001 791 90	0.002 025 81

TABLE III. Comparison of exact two-photon exchange calculation with MBPT: $Z=30$.

	$2\,^3S_1$	$2\,^3P_0$	$2\,^3P_2$
2γ	−0.049 550 08	−0.088 607 03	−0.075 275 12
MBPT	−0.049 541 34	−0.088 752 05	−0.075 352 75
QED	−0.000 008 74	0.000 145 02	0.000 077 63

TABLE IV. Comparison of exact two-photon exchange calculation with MBPT: $Z=40$.

	$2\,^3S_1$	$2\,^3P_0$	$2\,^3P_2$
2γ	−0.051 309 68	−0.102 226 23	−0.077 006 51
MBPT	−0.051 317 15	−0.102 742 32	−0.077 298 42
QED	−0.000 007 47	0.000 516 09	0.000 291 91

TABLE V. Comparison of exact two-photon exchange calculation with MBPT: $Z=50$.

	$2\,^3S_1$	$2\,^3P_0$	$2\,^3P_2$
2γ	−0.053 698	−0.121 820	−0.079 182
MBPT	−0.053 762	−0.123 159	−0.079 949
QED	0.000 064	0.001 340	0.000 767

TABLE VI. Comparison of exact two-photon exchange calculation with MBPT: $Z=60$.

	$2\,^3S_1$	$2\,^3P_0$	$2\,^3P_2$
2γ	−0.056 799	−0.149 366	−0.081 771
MBPT	−0.057 023	−0.152 243	−0.083 427
QED	0.000 224	0.002 877	0.001 656

TABLE VII. Comparison of exact two-photon exchange calculation with MBPT: $Z=70$.

	$2\,^3S_1$	$2\,^3P_0$	$2\,^3P_2$
2γ	−0.060 812	−0.187 937	−0.084 734
MBPT	−0.061 312	−0.193 398	−0.087 903
QED	0.000 500	0.005 460	0.003 168

TABLE VIII. Comparison of exact two-photon exchange calculation with MBPT: $Z=80$.

	$2\,^3S_1$	$2\,^3P_0$	$2\,^3P_2$
2γ	−0.065 988	−0.242 396	−0.088 127
MBPT	−0.066 954	−0.251 982	−0.093 609
QED	0.000 966	0.009 586	0.005 482

grals were evaluated by Gaussian methods, with the first point always a finite distance from the singularity, which served as a regulator. As long as the same order Gaussian was used to evaluate the canceling terms, the sum was well defined. The finite remainder of all such terms was numerically quite small, and scaled as $(Z\alpha)^5$, as was found in the ground-state case.

The nondivergent reference-state terms were found to be much larger. This is in contrast to the ground-state case, where even before inclusion of the reference-states, very close agreement between MBPT and the calculation was found. For the excited-state case, however, significant discrepancies between MBPT and the *S*-matrix calculation without reference states are present. This is because of our use of the Feynman gauge, which gives cut structure to photons with timelike indices: in the Coulomb gauge such photons have no cut structure, and do not contribute to the reference states. A breakdown of the reference-state contributions is given in Table II.

While many methods have been applied to the calculation of the structure of highly charged ions, one that is particularly closely related to the *S*-matrix approach of this paper is MBPT. Had we carried out the calculation in the Coulomb gauge, it would have been straightforward to show that, when both photons are Coulomb photons (C) and negative energy states are neglected, the energy calculated with the methods of this paper precisely reproduces the second-order energy $E^{(2)}$ of MBPT [11]. The neglected negative energy state terms are QED effects that scale as $(Z\alpha)^3$ a.u. at low Z. When one or both of the photons is a transverse photon (T), magnetic effects are involved. An approximate way of including them, often used in MBPT and configuration interaction (CI) [12] calculations, is to treat the instantaneous Breit interaction as a perturbation, again neglecting negative energy states. It is of interest to compare second-order MBPT, which we define to be the sum of $E^{(2)}$ (CC), $B^{(2)}$ $(CT+TC)$, and $B\times B$ (TT), with the present calculation.

We do this for $Z=30$, 40, 50, 60, 70, 80, and 92 in Tables III–IX, where the two-photon calculation of this paper is given in the row labeled ‘‘2γ,’’ second-order MBPT (with partial wave expansion limits chosen to be identical to the 2γ) given in the row labeled ‘‘MBPT,’’ and the difference labeled ‘‘QED.’’ It is important to note that this is just a convention: QED encompasses all of atomic physics, but here we are defining it to be the physics beyond that described by a many-body Hamiltonian with neglect of negative energy states and retardation.

The most notable feature of the two methods of calculation is their relatively close agreement. Even for the $2\,^3P_0$ state of heliumlike uranium, where the QED correction is largest, it is only a 0.5 eV effect, which is to be compared to the 8 eV experimental uncertainty [13]. This then explains why the procedure of calculating energy levels of highly charged ions by first applying relativistic MBPT, or the essentially equivalent CI method, is relatively successful: while in principle a full QED treatment, such as presented here, should be given, the extra physics is relatively small. However, experiments on heliumlike uranium accurate to several tenths of an eV are possible [14], and these will require the kind of QED treatment presented here.

TABLE IX. Comparison of exact two-photon exchange calculation with MBPT: $Z=92$.

	$2\,^3S_1$	$2\,^3P_0$	$2\,^3P_2$
2γ	−0.074 246	−0.340 886	−0.092 692
MBPT	−0.076 230	−0.358 222	−0.102 548
QED	0.001 984	0.017 336	0.009 856

At lower Z, the QED effects are smaller, but on the other hand the experiments are more accurate. We mention in particular experiments on heliumlike argon [15], which are accurate to 22 microHartrees. This is just at the level of the QED effect in the $2\,^3P_0$ state if the approximate scaling of Z^4 is used to extrapolate from $Z=30$ down to $Z=18$. However, until the related vertex diagrams are carried out, as has been recently done for lithiumlike ions [16], comparison with experiment cannot be made. Of particular note is the Z dependence of the QED effects. The change in sign between $Z=40$ and $Z=50$ present for the $2\,^3S_1$ state can be understood as an as yet uncalculated $(Z\alpha)^4$ overwhelming a known $(Z\alpha)^3$ contribution of

$$\Delta E_Q=-\frac{7(Z\alpha)^3}{6\pi}\left\langle\frac{1}{r_{12}^3}\right\rangle, \qquad (63)$$

where $1/r_{12}^3=0.013\,142$.

This allows a complementary approach to the determination of contributions of order α^4 a.u. in neutral helium, a problem that has been addressed using effective Hamiltonian methods [17]. However, before the accurate fits required to compare with the known low-Z behavior can be carried out, better control of the partial wave expansion is needed: it is necessary to carry out an extrapolation of the expansion to infinity, which we have not done in this paper. We estimate that to do this accurately will require the calculation of about 10 more partial waves, which is difficult to do with finite basis-set methods. However, differential equation methods allow much higher values of angular momentum to be accurately treated, and the next step of this calculation is the application of such methods to heliumlike ions with smaller nuclear charges.

ACKNOWLEDGMENTS

This work was supported in part by NSF Grant No. PHY-98-70017. We gratefully acknowledge very useful conversations with Dr. S. Blundell and Dr. A. E. Livingston. We also thank Dr. V. Shabaev for communications regarding the mixed-state problem.

[1] P.J. Mohr, Phys. Rev. A **32**, 1949 (1985), and references therein.
[2] S.A. Blundell, W.R. Johnson, P.J. Mohr, and J. Sapirstein, Phys. Rev. A **48**, 2615 (1993).
[3] Ingvar Lindgren, Hans Persson, Sten Salomonson, and Leonti Labzowsky, Phys. Rev. A **51**, 1167 (1995).
[4] H. Persson, S. Salomonson, P. Sunnergren, and I. Lindgren, Phys. Rev. Lett. **76**, 204 (1996); V.A. Yerokhin, A.N. Artemyev, and V.M. Shabaev, Phys. Lett. A **234**, 361 (1997).
[5] R.E. Marrs, S.R. Elliott, and Th. Stöhlker, Phys. Rev. A **52**, 3577 (1995).
[6] V.M. Shabaev and I.G. Fokeeva, Phys. Rev. A **49**, 4489 (1994).
[7] V.M. Shabaev (private communication).
[8] J. Sapirstein, K.T. Cheng, and M.H. Chen, Phys. Rev. A **59**, 259 (1999).
[9] J. Sapirstein and W.R. Johnson, J. Phys. B **29**, 5213 (1996).
[10] This has been done using a Green's-function approach by V. Shabaev (unpublished).
[11] J. Sapirstein, Rev. Mod. Phys. **70**, 55 (1998).
[12] K.T. Cheng, M.H. Chen, W.R. Johnson, and J. Sapirstein, Phys. Rev. A **50**, 247 (1994).
[13] C.T. Munger and H. Gould, Phys. Rev. Lett. **57**, 2927 (1986).
[14] A.E. Livingston (private communication).
[15] K. Kukla *et al.*, Phys. Rev. A **51**, 1905 (1995).
[16] V.A. Yerokhin *et al.*, Phys. Rev. A **60**, 3522 (1999).
[17] K. Pachucki, J. Phys. B **31**, 2489 (1998).